Dynamic scaling of out-of-plane fluctuations in freestanding graphene

Enzo Granato, Michelle Greb, K. R. Elder, S. C. Ying, and T. Ala-Nissila

Dynamic scaling of out-of-plane fluctuations in free-standing graphene

Enzo Granato,[1,2] Michelle Greb,[3] K. R. Elder,[3] S.C. Ying,[2] and T. Ala-Nissila[4,2,5]

[1]*Instituto Nacional de Pesquisas Espaciais,12227-010 São José dos Campos, SP, Brazil*
[2]*Department of Physics, P.O. Box 1843, Brown University, Providence, RI 02912-1843, USA*
[3]*Department of Physics, Oakland University, Rochester, Michigan 48309, USA*
[4]*QTF Centre of Excellence, Department of Applied Physics,*
Aalto University School of Science, P.O. Box 11000, FI-00076 Aalto, Espoo, Finland
[5]*Interdisciplinary Centre for Mathematical Modelling, Department of Mathematical Sciences,*
Loughborough University, Loughborough, Leicestershire LE11 3TU, UK

We study the dynamical behavior of the mean-square displacement of height fluctuations of free-standing graphene using a phase-field-crystal model introduced recently. We find that the dynamic scaling behavior obtained numerically at long times is well described by scaling theory of polymerized membranes. The critical exponent characterizing the power-law increases with time and depends only on the equilibrium roughening exponent ξ as $\alpha = \xi/(1+\xi)$. For sufficiently long times it crosses over to linear behavior for finite-size systems. The critical exponent α is in good agreement with the anomalous diffusion exponent observed experimentally in graphene, suggesting this is a property that could also be observable in other two-dimensional crystalline materials.

I. INTRODUCTION

The dynamics of flexible two-dimensional (2D) materials has recently received considerable attention. Of particular interest is free-standing graphene, which has many potential technological applications [1–5]. Its high degree of mechanical deformability induces significant flexural modes that can e.g. control thermal conduction in free-standing pristine graphene [6]. While the effects of thermal fluctuations have been studied by different approaches [1, 2, 5, 7–11], there is still lack of detailed and fundamental understanding of the dynamical behavior of such fluctuations [1, 3–5, 12, 13]. Accurate measurements have been performed on the mean-square height displacement [1] induced by thermal fluctuations, with scanning tunneling microscopy (STM). Surprisingly, the time dependence of height fluctuations has revealed anomalous sub-diffusive behavior at long times t, with a power law behavior t^α and $\alpha \approx 0.3$. Since out-of-plane fluctuations of graphene can be well described by elastic membrane models [7, 8, 14], an interesting question concerns the possible universality of such dynamic behavior. If this were the case, this behavior should not depend on the microscopic details. The value of α would then be constrained by the more fundamental roughening and dynamical critical exponents ξ and z. They characterize the power-law increase of the mean-square out-of-plane fluctuations as $L^{2\xi}$, and their crossover time as L^z, for a system of linear size L.

To examine these phenomena we use here a phase-field-crystal (PFC) model of 2D graphene that incorporates out-of-plane deformations in addition to in-plane deformations while still maintaining atomic resolution. Previously 2D PFC models have been used to study a variety of phenomena of atomistically thin films, including Moiré patterns, grain boundary energies, triple junction energies and polycrystals in graphene [15–17], and inversion boundaries and the formation and dynamics of defects in hexagonal boron nitride (hBN) [18, 19]. Such models have also been used to study thermal fluctuations effects in adsorbed layers [20, 21]. These models were able to predict grain boundary energies and structures, dislocation and inversion boundary energies and motion in overall agreement with molecular dynamics, quantum-mechanical density functional theory and experiments. Recently, a PFC model of layered materials was introduced specifically for graphene and hBN and bilayers of such systems [22]. For an atomistically thin layer, the PFC model with out-of-plane deformations describes the system by two coupled continuous fields, one representing the particle density and the other height fluctuations with a small amplitude. Thus, such a model is particularly suitable for the study of universal dynamical properties of crystalline membranes, such as free-standing graphene.

In the present work we thus focus on the dynamical behavior of free-standing graphene using the PFC model with out-of-plane deformations as mentioned above. The numerical simulations of the mean-square height displacement fluctuations show that at sufficient long times in finite systems the behavior is diffusive with $\alpha = 1$, but at intermediate times the exponent corresponds to sub-diffusive behavior with $\alpha < 1$. We find that this behavior can be described by a dynamic scaling theory already developed for polymerized membranes [23]. The data for different system sizes collapse as predicted by the theory. For sufficient large systems, only the short-time and intermediate-time behavior would be observed within a limited time scale. Remarkably, the scaling theory also predicts that the exponent α is given analytically as $\alpha = \xi/(1+\xi)$, being independent on the particular type of dynamics. The results are in good agreement with the experimental observation of sub-diffusive behavior at long times in free-standing graphene [1]. It indicates that it is a universal property resulting from thermal fluctuations and the nonlinear coupling between in-plane and out-of-plane fluctuations that could also be observable in other 2D crystalline materials.

II. PFC MODEL WITH OUT-OF-PLANE DEFORMATIONS

We use the PFC approach to describe the free-standing graphene as a 2D membrane in thermal equilibrium, allowing for deformations out of the plane, in addition to in-plane deformations. The model is described by the effective Hamiltonian [22]

$$\frac{H}{c_{\mathrm{g}}} = \int d\vec{r}\,[(\frac{\Delta B}{2}n^2 + \frac{B_{\mathrm{x}}}{2}n(\nabla_s^2 + 1)^2 n + \frac{\tau}{3}\,n^3 + \frac{v}{4}\,n^4)$$
$$+\frac{1}{2}\kappa \int d\vec{r}' C(\vec{r}-\vec{r}')h(\vec{r})h(\vec{r}')], \qquad (1)$$

where $n(\vec{r})$ is density field and $h(\vec{r})$ is the height displacement measured from a base plane with $\vec{r} = (x,y)$, and c_{g} is an energy-scale parameter. In Fourier space, $C(k) = k^4$ for $k < k_{\max}$ and $C(k) = C_{\max}$ for $k > k_{\max}$. Values of $C_{\max}$ and $k_{\max}$ are chosen to eliminate small scale fluctuations of $h(\vec{r})$. The surface Laplacian is approximated by

$$\nabla_s^2 \approx \nabla_{xy}^2 - (h_x^2\partial_x^2 + h_y^2\partial_y^2 + 2h_x h_y \partial_x \partial_y), \qquad (2)$$

assuming a small gradient expansion of $h(\vec{r})$, where $h_x = \partial h/\partial x$ and $h_y = \partial h/\partial y$. The values of the parameters entering Eq. (1) were chosen to model graphene [22] and are given in Sec. IV. The parameter ΔB largely controls the transition from liquid to crystalline states. The second term in Eq. (1) leads to the emergence of periodic equilibrium states and is responsible for in-plane elasticity. For $\tau > 0$ ($\tau < 0$), the equilibrium have honeycomb (triangular) symmetry. The last term controls the bending energy of the sheet.

The time evolution is obtained from dissipative dynamics, which drives the system to the minimum of the free energy functional. The dynamics of the density field n is conservative,

$$\frac{\partial n_h}{\partial t} = \nabla^2 \frac{\delta H}{\delta n_h} + \eta_n(r,t), \qquad (3)$$

while it is non-conservative for the height field h,

$$\frac{\partial h}{\partial t} = -\frac{\delta H}{\delta h} + \eta_h(r,t), \qquad (4)$$

where η_n and η_h are white noise terms describing the effects of thermal fluctuations [20] at temperature T, with zero mean and

$$\langle \eta_n(\vec{r},t)\eta_n(\vec{r}',t')\rangle = 2T\nabla^2\delta(\vec{r}-\vec{r}')\delta(t-t'), \qquad (5)$$

$$\langle \eta_h(\vec{r},t)\eta_h(\vec{r}',t')\rangle = 2T\delta(\vec{r}-\vec{r}')\delta(t-t'), \qquad (6)$$

As shown previously [22], the model reduces to the continuous elastic model used to study flexible sheets [24] in the limit of small deformations. In this limit and $T = 0$, the stationary solutions of these equations correspond to the minimization of the energy functional of Eq. (1),

leading to the von-Karman equation equations for bending of thin plates [25].

The numerical simulations described in Sec. IV were performed mainly with conservative dynamics for $n(r)$ but additional calculations used non conservative dynamics analogous to Eq. (4).

III. DYNAMIC FINITE-SIZE SCALING

The scaling theory for the mean-square displacement of height fluctuations has already been considered in the context of polymerized membranes [23]. Fluctuations can be described by an elasticity theory where the in-plane and out-of-plane deformations are coupled by a nonlinear term [24, 26]. The combined effect of this coupling and thermal fluctuations leads to the mean-square fluctuations out of the plane of the membrane, $\langle h_{\mathrm{p}}^2 \rangle$, increasing with system size L as a power law $\langle h_{\mathrm{p}}^2 \rangle \propto L^{2\xi}$, with the roughening exponent $\xi \approx 0.6$ significantly different from its value in absence of the nonlinear coupling, $\xi = 1$. The time evolution of the mean-square height displacement $\langle \Delta h(t)^2 \rangle = \langle (h(r,t_0+t) - h(r,t_0))^2 \rangle$ can be divided in three different regimes. For short times, the behavior depends on the details of dynamics at short length scales and is not expected to be universal. On the other hand, at intermediate and long times it does not depend on the microscopic length, although it can still depend on the type of dynamics. As in critical phenomena, one then expects that at intermediate and long times it should satisfy the scaling form [23]

$$\langle \Delta h(t)^2 \rangle = L^{2\xi}\Phi(t/L^z), \qquad (7)$$

where z a the dynamic critical exponent. In a finite system with free boundary conditions, the center-of-mass diffusion is the dominant contribution in the long time regime, leading to a linear behavior $\langle \Delta h(t)^2 \rangle \sim D_{\mathrm{cm}}t$, where D_{cm} is the diffusion coefficient and thus the scaling function $\Phi(x) \propto x$ for large x. Moreover, since $D_{\mathrm{cm}} \propto 1/L^2$, the dynamic exponent is constrained to

$$z = 2(1+\xi). \qquad (8)$$

In the intermediate time regime, where the behavior is size-independent, the scaling function should behave as $\Phi(x) \sim x^{2\xi/z}$. Then from Eq. (8) the scaling form implies that $\langle \Delta h(t)^2 \rangle \propto t^{2\xi/z} \sim t^\alpha$ with the critical exponent given by

$$\alpha = \frac{\xi}{(1+\xi)}. \qquad (9)$$

This sub-diffusive behavior corresponding to $\alpha < 1$ results from the collective effects of internal modes, which dominate the dynamical behavior at the intermediate time regime.

A notable feature of the scaling relation of Eq. (9) is that α depends only the critical exponent ξ, which is a

static equilibrium property. This is a consequence of the scaling relation (8) for the dynamical exponent z, which is determined by ξ, rather than being an independent critical exponent. Therefore, α is independent of the details of the particular dynamics chosen to model the time evolution of the system. Other properties, however, may depend on the dynamics.

We find it useful to include the temperature T explicitly in the scaling form. Assuming that the center-of-mass diffusion constant obeys the usual Einstein's relation, $D_{cm} = T\mu$, where μ is the mobility, and that $\langle h^2 \rangle \propto TL^{2\xi}$, as obtained from harmonic elasticity theory [26], the same arguments above lead to the scaling form

$$\langle \Delta h(t)^2 \rangle = TL^{2\xi}\Phi(t/L^z). \tag{10}$$

In the Appendix, we demonstrate this scaling form in absence of the nonlinear coupling between in-plane and out-of-plane deformations, corresponding to $B_x = 0$ in Eq. (1), and also show that in the presence of this coupling the linear behavior $\langle \Delta h(t)^2 \rangle \propto T\,t$ remains valid in the long-time regime.

For the experiments on graphene, the scaling theory should be valid in the temperature regime where topological defects are absent. This condition is well satisfied since experiments are usually performed around room temperature [1], where the thermal energy is much smaller than the excitation energy of such defects. Moreover, since from Eqs. (7) and (10), the crossover time τ, where the long time behavior of linear diffusion sets in, scales as

$$\tau \propto L^z, \tag{11}$$

only the intermediate time behavior is observed for large systems within the limited experimental time scale, with the power-law behavior $\langle \Delta h(t)^2 \rangle \sim t^\alpha$. Thus the critical exponent α given by Eq. (9) corresponds to the anomalous diffusion exponent observed at long times in the experiments. Using the value of ξ obtained from Monte Carlo simulations of graphene [7] $\xi = 0.575$, we obtain $\alpha = 0.365$, which is in good agreement with the anomalous exponent found experimentally [1]. In the next section, we present numerical simulation results from the PFC model of Eq. (1) providing support to the scaling forms of Eqs. (7) and (10) for free-standing graphene.

IV. NUMERICAL SIMULATIONS

The coupled Eqs. (3) and (4) are solved numerically in Fourier space [22] with wave vector $\vec{k}$, as a function of time t with time step Δt. A square lattice is used of linear size $L\Delta x$ with periodic boundary conditions and mesh size $\Delta y = \Delta x$. To eliminate small-scale fluctuations of $n(\vec{r})$, $\eta_n(k,t)$ is set to zero for $k > k_{max}$. We set the PFC parameters to $\Delta B = -0.15$, $B_x = 1$, $\tau = -0.874818$, $v = 1$, $\kappa = 0.209726$ and $c_g = 6.58$ eV, which has

FIG. 1. Ground-state configuration (left) and representative configuration at $T = 0.004$ (right), corresponding to $\sim 300K$.

been shown previously to describe many properties of graphene in the ground state [22]. Dimensionless units are used in the Hamiltonian. The conversion factors for temperature and length are c_g/k_B and $0.353\mathring{A}$, respectively. However, it is not possible to convert time to physical units because the kinetic coefficients in the phenomenological equations, Eqs. (3) and (4), are arbitrary. The main results are obtained for mesh size $\Delta x \approx 0.5$, time step $\Delta t = 0.5$ and $k_{max} = 0.5$. In dimensionless units, room temperature corresponds to $T \approx 0.004$. Figure 1 illustrates the ground-state configuration and a typical configuration at $T = 0.004$. The numerical results described below were obtained at higher temperatures, $T \geq 0.02$, and system sizes up to $L = 250$ in order to reach thermal equilibrium and observe crossover behavior within the limited computer time. For this range of temperatures, the thermal length [27] above which nonlinear thermal fluctuations are expected to dominate corresponds to $L_{th} < 7$ Å, well below the systems sizes used in the numerical simulations (~ 50 Å) and experiments (~ 7 μm).

From the time dependence of the height fluctuations $h(r,t)$ at fixed value of $\vec{r}$, we computed its mean-squared displacement $\langle \Delta h(t)^2 \rangle = \langle ((h(r,t_0 + t) - h(r,t_0))^2 \rangle$ for different system sizes. The time average was performed after the initial ground-state configuration reached thermal equilibrium, which required typically 10^5 time steps. Figure 2 shows the time dependence for small systems ($L < 160$)) at $T = 0.04$. It displays three different regimes. The intermediate and long-time regimes can be characterized by power-law behavior $\langle \Delta h(t)^2 \rangle \sim t^\alpha$. For the smallest system at long times $\alpha \approx 1$, which is the conventional diffusive behavior. For the largest system $L = 160$, at intermediate times $\alpha \approx 0.35$, before crossing over to $\alpha \approx 1$ at long times. For much larger systems, crossover to the behavior with $\alpha \approx 1$ is not observed within the time available in the present calculation. For the short-time behavior $\alpha \approx 0.6$. We do not observe thermally excited topological defects, such as isolated dislocations for these system sizes. However, they are predicted to occur for sufficiently large systems due to the finite value of the dislocation energy [25].

The crossover from an intermediate time regime with subdiffusive dynamics to normal diffusion at long times is consistent with the dynamical scaling theory of equilibrium fluctuations [23] described in Sec. III. In Fig. 3 we show a scaling plot of $\langle \Delta h(t)^2 \rangle/L^{2\xi}$ vs. $t/L^{2(1+\xi)}$, according to Eqs. (7) and (8), containing a single adjustable
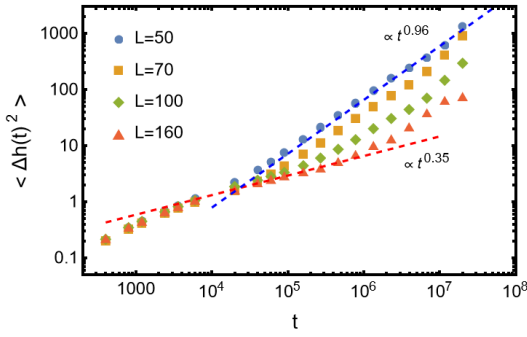
FIG. 2. Mean-squared height displacement $\langle \Delta h(t)^2 \rangle$ as a function of time t for different systems sizes L at $T = 0.04$. Dotted lines are are power-law fits, at intermediate times for $L = 160$ and at long times for $L = 50$.
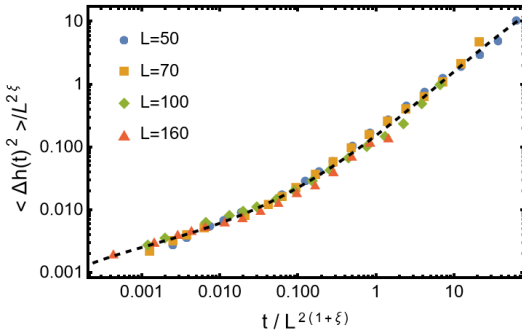

FIG. 3. Scaling plot of the data in the intermediate and long-time regimes from Fig. 2 according to Eq. (7) with $\xi = 0.62$.

parameter ξ. The best data collapse is obtained with the roughening exponent $\xi = 0.62(9)$ which is comparable with the previous estimates from Monte Carlo simulations of an atomistic model of graphene [7], $\xi = 0.575$. Simulations and analytical results for different models of fluctuating tethered membranes give values in the range [28] $\xi = 0.575 - 0.66$. The roughening exponent can also be obtained directly from the mean-square out-of-plane fluctuations $\langle h_p^2 \rangle = \langle h(r,t)^2 \rangle - \langle h(r,t) \rangle^2$, which is
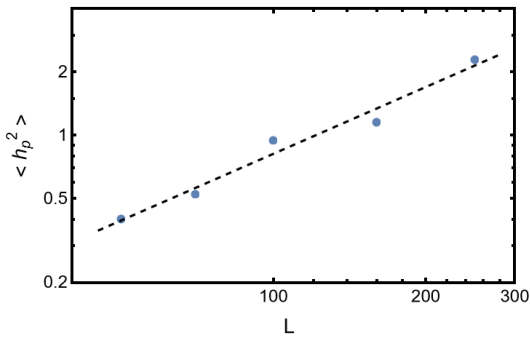

FIG. 4. Mean-square out-of-plane fluctuation as a function of system size at $T = 0.04$. The dotted line is a power law fit $\langle h_p(r,t)^2 \rangle \propto L^{2\xi}$ with $\xi = 0.53(5)$.
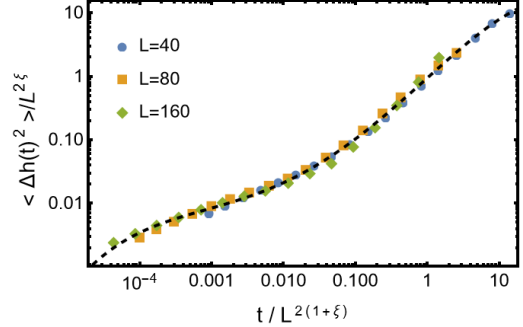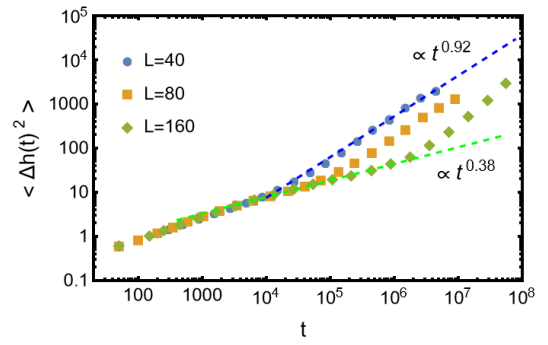

FIG. 5. (a) Mean square height displacement $\langle \Delta h(t)^2 \rangle$ as a function of time t for different systems sizes L, with non-conserved dynamics for $n(r)$ at $T = 0.4$. Dotted lines are a power-law fits at intermediate times for $L = 160$ and at long times for $L = 40$. (b) Scaling plot according to Eq. (7) with $\xi = 0.72$.

an equilibrium quantity and should scale with system size as [24, 26] $\langle h_p^2 \rangle \propto T L^{2\xi}$. As shown in Fig. 4, the size dependence of $\langle h_p^2 \rangle$ can be fitted to a power law giving the estimate $\xi = 0.53(5)$, consistent with the above estimate from the dynamic scaling. From Fig. 4, we estimate a typical out-of-plane fluctuation $\sqrt{\langle h_p^2 \rangle} \approx 5$ Å for a 1 μm sample at room temperature, which is in the range of measured values [1, 2, 7].

Additional results were obtained from simulations with non-conservative dynamics for $n(r)$, analogous to Eq. (4). According to the scaling relation of Eqs. (8) and (9), z and α depend only on the critical exponent ξ, which is a thermal equilibrium property. Therefore, they should be independent of the details of the particular dynamics. Indeed, as shown in Fig. 5 for $T = 0.4$, $\alpha = 0.72(9)$ and the scaling plot gives the same results as obtained above with conservative dynamics within the estimated errors.

From Eq. (9), the anomalous subdiffusion exponent is in the range $\alpha = 0.3 - 0.41$ using our above estimates of ξ. It is consistent with the one observed experimentally at long times [1], $\alpha \approx 0.3$, in measurements of vertical motion of atoms in free-standing graphene at room temperature. The absence of crossover to linear diffusion at long times indicates that the crossover time τ from
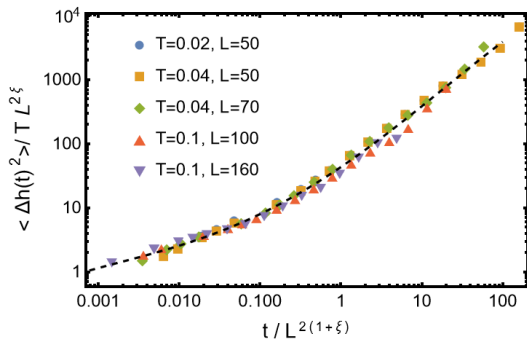
FIG. 6. Scaling plot including different temperatures, according to Eq. (10) with $\xi = 0.5$.
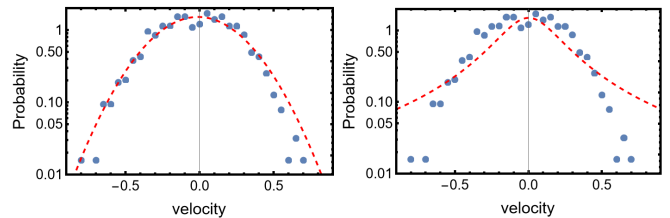

FIG. 7. Velocity probability distribution for $L = 160$ at $T = 0.04$, fitted to different analytical forms (dotted lines). Left panel: Red dashed line shows the Gaussian distribution $e^{-(v-v_0)^2/2\sigma^2}/\sigma\sqrt{2\pi}$. Right panel: Lorentzian distribution $(1/\pi\Gamma)/[1 + ((v - v_0)/\Gamma)^2]$. Velocity is in units of $(\Delta x/\Delta t) \times 10^{-4}$.

Eq. (11) is beyond the time scale of the experiment. Although the temperature here is much higher, additional calculations at different temperatures give similar results. In fact, data collapse is found for different temperatures according to Eq. (10) as shown by the scaling plot in Fig. 6, with $\xi = 0.5(1)$. Since the temperature appears just as a multiplicative factor in the scaling form of Eq. (10), the same crossover behavior should be observed at the lower temperature of the experiments.

There is a surprising finding in the experiments, however, that is not reproduced by the present simulations of the PFC model. The probability distribution of the membrane velocity obtained from the time dependence of the height displacement was found to be well described by a Lorentzian distribution [7]. Instead, we find that the velocity distribution is better described by a Gaussian, as shown in Fig. 7. This could be due to the pure relaxational dynamics described by Eqs. (3) and (4) which ignore, for example, inertial effects [21]. On the other hand, if the Lorentzian distribution results from mirror buckling events occurring at very large time scales [1, 5, 12, 13], as suggested by the atomistic calculations, these effects would not be observable in the numerical simulations. In the experimental work it was proposed that the anomalous exponent α is a consequence of such particular Lorentzian distribution. Nevertheless, since we find that α depends only ξ, which is an equilibrium property, it indicates that the anomalous α is not necessarily a consequence of a particular velocity distribution.

V. SUMMARY AND CONCLUSIONS

Thermally induced fluctuations of free-standing graphene were studied by a PFC model introduced recently [22], which incorporates out-of-plane deformations in addition to in-plane deformations. The mean square displacement of height fluctuations at sufficient long times in finite systems shows a linear diffusive behavior t^α with $\alpha = 1$, while at intermediate times the behavior is sub-diffusive, $\alpha < 1$. The crossover between the two different regimes and its dependence on system size

can be described by a dynamic scaling theory developed for polymerized membranes [23]. We have demonstrated that the data for different system sizes and temperatures collapse into a single curve as predicted by the scaling arguments. For sufficient large systems, only the short-time and intermediate-time behavior would be observed within a limited time scale, as found experimentally. If the experimental conditions prevent the center-of-mass diffusion at long times, the linear behavior is replaced by a saturation regime. While the short-time behavior is non-universal, the intermediate-time behavior is described by a universal critical exponent, given analytically as $\alpha = \xi/(1+\xi)$, in terms of the roughening critical exponents ξ, being independent on the particular type of dynamics. These results are in good agreement with the experimental observation of sub-diffusive behavior at long times with $\alpha \approx 0.3$ in free-standing graphene [1] and could also be observable in many other two-dimensional crystalline materials. The model presented in this paper can also be used to study defected systems, such as polycrystals, as was also done in earlier work [22] and by Zhang et. al. [29]. It would interesting to examine the influence of defects on the height fluctuations in such models.

VI. ACKNOWLEDGEMENTS

Appendix A

To give context to the results presented in this paper it is convenient to consider the limit in which Eq. (4), which explicitly reads,

$$\frac{\partial h}{\partial t} = -\kappa \nabla^4 h - 2\vec{\nabla} \cdot \vec{N} + \eta_h \qquad (A1)$$

where $\vec{N} = [\vec{\nabla} h \cdot \vec{\nabla}(\vec{\nabla} n)](1 + \nabla_s^2)n$ is linearized, i.e.,

$$\frac{\partial h}{\partial t} = -\kappa \nabla^4 h + \eta_h. \qquad (A2)$$

Equation (A2) has a solution for an initial condition $h(\vec{r}, 0) = 0$ in Fourier space

$$\hat{h}(\vec{k}, t) = e^{-\kappa k^4 t} \int_0^t dt' e^{\kappa k^4 t'} \hat{\mu}_h(\vec{k}, t'), \qquad (A3)$$

where $\hat{h}$ and $\hat{\mu}_h$ are the Fourier transforms of h and μ_h respectively.

The mean square displacement is then

$$\langle \Delta h^2(t) \rangle = \frac{2T}{(2\pi)^2} \int d\vec{k} \int_0^t dt' e^{-2\kappa k^4 (t-t')}, \qquad (A4)$$

where $\langle \hat{\mu}_h(\vec{k}', t') \hat{\mu}_h(\vec{k}, t) = 2T \delta_k(\vec{k}' + \vec{k}) \delta(t' - t)$ was used. Integrating in polar coordinates from $k = 2\pi/L$ to ∞ gives;

$$\langle \Delta h^2(t) \rangle = \frac{TL^2}{16\pi^3 \kappa} \left[\alpha \pi^{1/2} \mathrm{erf}(\alpha) + 1 - e^{-\alpha^2} \right], (A5)$$

where $\alpha \equiv 4\sqrt{2t\kappa}\pi^2/L^2$ and $\mathrm{erf}(x)$ is the error function. Thus in the small time limit $\alpha \ll 1$,

$$\langle \Delta h^2(t) \rangle = T\sqrt{\frac{t}{8\kappa\pi}} + \cdots, \qquad (A6)$$

valid in the limit $t \ll L^4/(32\kappa\pi^4)$. It can shown that if $h(r, 0)$ were an equilibrium solution, the same time dependence would emerge. For the $k = 0$ mode, which

corresponds to the average of h, a different result is obtained. In this case

$$\langle \Delta h^2(t) \rangle = 2T \frac{1}{L^2} \int_0^t dt' \int_0^t dt'' \delta(t - t')$$
$$= 2Tt/L^2, \qquad (A7)$$

consistent with the temperature scaling shown in Fig. 6. It is interesting to note that the non-linear contributions to Eq. (A1) are zero in the $k = 0$ limit, thus Eq. (A7) should be valid for Eq. (4). The simplified Eq. (A2) also has a prediction for the mean average square $\langle h(\vec{r}, t)^2 \rangle$ in the infinite time limit, i.e.,

$$\langle h(\vec{r}, t)^2 \rangle = \frac{T}{\kappa} \int \frac{d\vec{k}}{(2\pi)^2} \frac{1 - e^{-2\kappa k^4 t}}{k^4}. \qquad (A8)$$

In the infinite time limit, integrating from $k = 2\pi/L$ to ∞ then gives

$$\langle h(\vec{r}, \infty)^2 \rangle = \frac{TL^2}{8\kappa\pi^3}, \qquad (A9)$$

implying an exponent of $\xi = 1$.

If the more general equation,

$$\frac{\partial h}{\partial t} = (-1)^{\beta+1} \nabla^{2\beta} h + \eta_h \qquad (A10)$$

is considered, where β is an integer greater than one, it is straightforward to show that

$$\langle h(\vec{r}, \infty)^2 \rangle \sim TL^{2(\beta-1)}/\kappa \qquad (A11)$$

which gives $\xi = \beta - 1$. Additionally by dimensional analysis Eq. (A10) gives,

$$t \sim L^{2\beta} \sim L^{2(1+\xi)}, \qquad (A12)$$

implying an exponent $z = 4$ and justifying the scaling in Figs. 3 and 5.

[1] M. Ackerman, P. Kumar, M. Neek-Amal, P. Thibado, F. Peeters, and S. Singh, Anomalous dynamical behavior of freestanding graphene membranes, Physical Review Letters **117**, 126801 (2016).

[2] J. C. Meyer, A. K. Geim, M. I. Katsnelson, K. S. Novoselov, T. J. Booth, and S. Roth, The structure of suspended graphene sheets, Nature **446**, 60 (2007).

[3] P. G. Steeneken, R. J. Dolleman, D. Davidovikj, F. Alijani, and H. S. Van Der Zant, Dynamics of 2d material membranes, 2D Materials (2021).

[4] P. Thibado, P. Kumar, S. Singh, M. Ruiz-Garcia, A. Lasanta, and L. Bonilla, Fluctuation-induced current from freestanding graphene, Physical Review E **102**, 042101 (2020).

[5] M. Neek-Amal, P. Xu, J. Schoelz, M. Ackerman, S. Bar-

ber, P. Thibado, A. Sadeghi, and F. Peeters, Thermal mirror buckling in freestanding graphene locally controlled by scanning tunnelling microscopy, Nature communications **5**, 1 (2014).

[6] Z. Fan, L. F. C. Pereira, P. Hirvonen, M. M. Ervasti, K. R. Elder, D. Donadio, T. Ala-Nissila, and A. Harju, Thermal conductivity decomposition in two-dimensional materials: Application to graphene, Physical Review B **95**, 144309 (2017).

[7] J. Los, M. I. Katsnelson, O. Yazyev, K. Zakharchenko, and A. Fasolino, Scaling properties of flexible membranes from atomistic simulations: application to graphene, Physical Review B **80**, 121405 (2009).

[8] A. Fasolino, J. Los, and M. I. Katsnelson, Intrinsic ripples in graphene, Nature materials **6**, 858 (2007).

[9] F. Ahmadpoor, P. Wang, R. Huang, and P. Sharma, Thermal fluctuations and effective bending stiffness of elastic thin sheets and graphene: A nonlinear analysis, Journal of the Mechanics and Physics of Solids **107**, 294 (2017).

[10] D. Wan, D. R. Nelson, and M. J. Bowick, Thermal stiffening of clamped elastic ribbons, Physical Review B **96**, 014106 (2017).

[11] A. Morshedifard, M. Ruiz-García, M. J. A. Qomi, and A. Košmrlj, Buckling of thermalized elastic sheets, Journal of the Mechanics and Physics of Solids **149**, 104296 (2021).

[12] Y. Kai, W. Xu, B. Zheng, N. Yang, K. Zhang, and P. Thibado, Origin of non-gaussian velocity distribution found in freestanding graphene membranes, Complexity **2019** (2019).

[13] J. M. Mangum, F. Harerimana, M. N. Gikunda, and P. M. Thibado, Mechanisms of spontaneous curvature inversion in compressed graphene ripples for energy harvesting applications via molecular dynamics simulations, Membranes **11**, 516 (2021).

[14] D. Nelson, T. Piran, and S. Weinberg, *Statistical mechanics of membranes and surfaces* (World Scientific, 2004).

[15] M. Smirman, D. Taha, A. K. Singh, Z.-H. Huang, and K. R. Elder, Phys. Rev. B **95**, 085407 (2017).

[16] P. Hirvonen, Z. Fan, M. M. Ervasti, H. Ari, E. K.R., and T. Ala-Nissila, Sci. Rep. **7**, 4754 (2017).

[17] P. Hirvonen, M. M. Ervasti, Z. Fan, M. Jalalvand, M. Seymour, S. M. V. Allaei, N. Provatas, A. Harju, K. R. Elder, and T. Ala-Nissila, Multiscale modeling of polycrystalline graphene: A comparison of structure and defect energies of realistic samples from phase field crystal models, Physical Review B **94**, 035414 (2016).

[18] D. Taha, S. K. Mkhonta, K. R. Elder, and Z.-F. Huang, Phys. Rev. Lett. **118**, 255501 (2017).

[19] D. Taha, S. R. Dlamini, S. K. Mkhonta, K. R. Elder, and Z.-F. Huang, Phys. Rev. Matt. **3**, 095603 (2019).

[20] J. Ramos, E. Granato, C. Achim, S. Ying, K. Elder, and T. Ala-Nissila, Thermal fluctuations and phase diagrams of the phase-field crystal model with pinning, Physical Review E **78**, 031109 (2008).

[21] J. Ramos, E. Granato, S. Ying, C. Achim, K. Elder, and T. Ala-Nissila, Dynamical transitions and sliding friction of the phase-field-crystal model with pinning, Physical Review E **81**, 011121 (2010).

[22] K. Elder, C. Achim, V. Heinonen, E. Granato, S. Ying, and T. Ala-Nissila, Modeling buckling and topological defects in stacked two-dimensional layers of graphene and hexagonal boron nitride, Physical Review Materials **5**, 034004 (2021).

[23] K.-I. Mizuochi, H. Nakanishi, and T. Sakaue, Dynamical scaling of polymerized membranes, EPL (Europhysics Letters) **107**, 38003 (2014).

[24] D. Nelsonand L. Peliti, Fluctuations in membranes with crystalline and hexatic order, Journal de Physique **48**, 1085 (1987).

[25] H. S. Seungand D. R. Nelson, Defects in flexible membranes with crystalline order, Physical Review A **38**, 1005 (1988).

[26] P. Chaikinand T. Lubensky, *Principles of condensed matter physics* (Cambridge University Press, Cambridge (GB), 1995).

[27] S. Shankarand D. R. Nelson, Thermalized buckling of isotropically compressed thin sheets, Physical Review E **104**, 054141 (2021).

[28] A. Tröster, High-precision fourier monte carlo simulation of crystalline membranes, Physical Review B **87**, 104112 (2013).

[29] T. Zhang, X. Li, and H. Gao, Designing graphene structures with controlled distributions of topological defects: A case study of toughness enhancement in graphene ruga, Extreme Mechanics Letters **1**, 3 (2014).